Influence of Exothermic Interaction on the Morphology and Droplet Coalescence of Melt-Mixed Immiscible Polymer Blends Containing a Block Copolymer

Jong Ryang Kim, Alex M. Jamieson,* Steven D. Hudson, Ica Manas-Zloczower, and Hatsuo Ishida

Department of Macromolecular Science, Case Western Reserve University, Cleveland, Ohio 44106

Received December 30, 1997; Revised Manuscript Received May 27, 1998

ABSTRACT: We investigate morphology evolution under melt blending of an immiscible mixture of two polymers, to which small amounts of a block copolymer are added as an emulsifier. We demonstrate the effect on blend morphology of an exothermic interaction between the major component, which constitutes the continuous matrix, and the compatible segment of the block copolymer. The system studied comprises poly(styrene-*co*-acrylonitrile) (SAN) as the matrix, poly(cyclohexyl methacrylate) (PCHMA) as the minor component, and poly(styrene-*b*-methyl methacrylate) (PS-*b*-PMMA) as the emulsifier. The degree of exothermic interaction between the SAN random copolymer and the PMMA segment of PS-*b*-PMMA was increased by changing the acrylonitrile content from 33% to 26%. To facilitate migration of the block copolymer to the blend interface, it was first coprecipitated with the minor phase and then dry-mixed with the major component. The spatial distribution of the PS-*b*-PMMA could be observed by selective staining of the PS segment, thereby allowing qualitative analysis of the surface activity of the block copolymer. The specimens were subjected to shear mixing in parallel plate geometry at a high shear rate to produce small droplet sizes, and then droplet coalescence was observed subsequently at a low shear rate. The addition of a block copolymer decreases the rate of droplet coalescence. The emulsified blend containing SAN26 had smaller droplets under high shear and slower droplet coalescence under low shear. These observations are consistent with the dual expectation that the exothermic mixing increases the swelling of the PMMA segment, which lowers interfacial tension, and leads to a more rigid interface.

Introduction

It is well-known that addition of a block copolymer (bcp) is effective in emulsifying immiscible polymer blends. The morphology of such blends prepared by solvent casting is determined by thermodynamic factors which control the lowering of interfacial tension. In previous work,[1] we have demonstrated that effective emulsification is determined by the balance between the swelling of the bcp segments on either side of the phase boundary. Such swelling is enhanced when the segment molecular weight is larger than that of the compatible homopolymer and if there is an exothermic interaction between them.[1−3] For effective emulsification of the minor component, the swelling between the major component and the compatible segment must be larger than that of the corresponding interaction involving the minor component. However, if the imbalance in swelling is too large, emulsification breakdown occurs[1,3] because the disperse-phase domains become too small to accommodate all of the minor component, unless more bcp is added.

The role of bcp in emulsifying immiscible polymer blends prepared by melt mixing is more obscure. In addition to the thermodynamic influence of the bcp, kinetic effects become important. For example, the presence of a small amount of a block copolymer can prevent coalescence of dispersed droplets during the melt-mixing process.[4,5] Originally, this phenomenon was explained as a further consequence of the fact that the block copolymer acts to reduce the interfacial energy between the two phases. Recently, however, it was suggested that migration of the block copolymer to the interface will stabilize droplets by imparting the ability to immobilize the interface.[6−8] However, experimental efforts have not succeeded in confirming this mechanism.

The purpose of the present research effort is to gain further insight into the role of bcp in emulsifying immiscible blends prepared by melt mixing, by investigating the influence of an exothermic interaction between one of the phases and a segment of the block copolymer. The blend system selected for study consists of poly(styrene-*co*-acrylonitrile) (SAN) random copolymer as the major phase, poly(cyclohexyl methacrylate) (PCHMA), immiscible with SAN, as the minor phase, and poly(styrene-*b*-methyl methacrylate) block copolymer (bcp) as the emulsifier. In this blend, as in our earlier work on solvent-cast blends,[1,2] the degree of exothermic interaction between the SAN copolymer and the poly(methyl methacrylate) (PMMA) block of the bcp can be varied by changing the acrylonitrile (AN) content in the SAN copolymer. PCHMA, used as the minor phase, is immiscible with SAN within the range of AN content used (from 15% to 33%).[4] PCHMA is also immiscible with PMMA and is miscible with PS. The PS segment of a PS-*b*-PMMA diblock copolymer, used as the emulsifier, is stained dark with ruthenium tetroxide, whereas SAN is partially stained to a light gray image and PCHMA is unstained. This allows us to observe the phase morphology using transmission electron microscopy (TEM), and in particular the location of the bcp (Figure 1).

Blend morphologies are often studied after processing with extruders or mixers.[4,5,10−12] This involves complex deformation histories which are a combination of extension and shear, and a range of high and low deformation rates. Thus, morphologies generated under such com-

S0024-9297(97)01888-3 CCC: $15.00
Published on Web 07/23/1998

Table 1. Molecular-Weight Averages of Polymers Samples

name	acronym	M_n (k)	M_w (k)	M_w/M_n
PS-*b*-PMMA diblock copolymer[a]	bcp	143.8/154.8	160.5/173.4	1.12
poly(cyclohexyl methacrylate)[b]	PCHMA	38.5	133.6	3.47
styrene−acrylonitrile copolymer[c] (26% AN content)	SAN26	68.6	153.0	2.23
styrene−acrylonitrile copolymer[c] (33% AN content)	SAN33	66.7	130.1	1.95

[a] Purchased from Polymer Source Inc. [b] Purchased from Scientific Polymer Products. [c] Supplied by Mitsui Toatsu Chemicals Inc.

Table 2. Calculated Values of Flory−Huggins Parameter (χ), Interfacial Tension (Γ), and Droplet Size (D)

	SAN26/PCHMA		SAN33/PCHMA	
$\dot{\gamma}$ (s^{-1})	50	1	50	1
η_m (Pa·s)	1420	7210	1340	6130
η_d (Pa·s)	2910	12900	2910	12900
η_r	2.05	1.75	2.17	2.10
χ	0.0236		0.0473	
Γ (mN/m)	1.73		2.44	
D_{Taylor} (μm)[a]	0.022	0.21	0.032	0.35
D_{Grace} (μm)[b]	0.036	0.30	0.057	0.62
$D_{Experiment}$ (μm)	0.068	0.40	0.11	0.69

[a] Equation 3. [b] Equation 4.

plex deformation fields are difficult to interpret quantitatively in terms of their rheological history. In the present experiments, to avoid such difficulties, a simple shear deformation was utilized via rotating parallel plate geometry in a Rheometrics RMS 800 rheometer.

Experimental Section

Materials. The molecular weights and polydispersities of the materials used are presented in Table 1 with their acronyms. SAN copolymers available have AN contents of 15%, 26%, 29%, and 33%. Maximal exothermic mixing with PMMA occurs for SAN15 and the degree of exothermic mixing decreases with an increase in AN content to a minimum for SAN33. SAN15 is miscible with PCHMA and so cannot be used in the present study. In this paper, we investigate droplet breakup and coalescence behavior in SAN26/bcp/PCHMA and SAN33/bcp/PCHMA.

Sample Preparation. For preparation of polymer blends by solvent casting, solutions of SAN, PCHMA, and bcp were made up in MEK solvent at a concentration of 1 g/100 mL. The ternary blends containing SAN, PCHMA, and bcp were made by mixing stock solutions in appropriate amounts. The ratio of SAN to PCHMA was fixed at 8:2 and up to 5% of bcp was added to the blend system without changing that ratio. The solvent was slowly evaporated over 14 days at room temperature and the final solvent traces were removed by drying at 70 °C for 24 h at atmospheric pressure and drying under vacuum for another 24 h.

For melt blending in the rheometer, crude mixtures were first prepared by dry mixing the blend components in powder form. In preparing blends containing the bcp, the bcp and the minor phase constituent, PCHMA, were first dissolved in MEK solvent and coprecipitated and the precipitates were dried in a vacuum oven for 24 h at room temperature. This material in powder form was then dry mixed with the major phase. This procedure facilitates migration of the bcp to the phase boundary. The dry-mixed powders were molded to form disks at 200 °C under vacuum in a Carver Lab Press compression molding machine.

Viscosity Measurement. Apparent viscosities were measured at 200 °C for SAN26, SAN33, and PCHMA using the RMS 800 rheometer with parallel plate geometry. The samples show shear-thinning behavior. Values of the apparent viscosity, η_m and η_d for the matrix and droplet phases, respectively, at 1 and 50 s^{-1} are listed in Table 2.

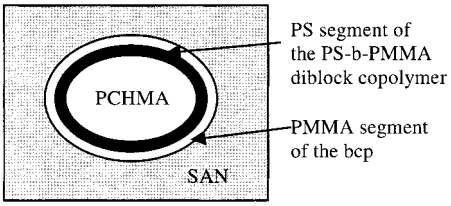

Figure 1. Schematic diagram for the image of blends by TEM.

Processing. Disk samples, prepared as described above, were sheared in parallel plate geometry with diameter 7.9 mm and gap 0.5 mm at 200 °C, using the RMS 800 rheometer. Shearing was first performed at a higher shear rate of 50 s^{-1}, to produce breakup of large droplets of the minor phase. After the samples underwent shearing at 50 s^{-1} for a specified time, a low shear rate of 1 s^{-1} was applied suddenly to allow shear-induced coalescence of the small droplets. The samples were cooled after 1 min of equilibration time followed by the rapid cooling mode with liquid nitrogen. The time required for the temperature to fall from the processing condition at 200 °C to the point at which the glass transition occurs (∼100 °C) was 30 s. This is believed to be short enough to quench and freeze the original morphology.

Analysis. JEOL 100 SX or 100 CX TEM with an acceleration voltage of 100 kV was used to investigate the morphologies of blends by melt blending and solvent casting. For TEM observation to investigate the maximum shear region of the sample, the edge perimeter areas of the melt-blended disk specimens were sectioned into ultrathin films of 50−80 nm thickness using a diamond knife and a RMC Inc. MT-7000 ultramicrotome machine. Sectioned films were exposed to RuO_4 vapor for 14 min in an enclosed chamber containing 0.25% aqueous solution of RuO_4. The PS segment of the bcp and the SANs are stained with RuO_4 such that the PS segment is seen as the darkest image, and the SAN major phase is light gray as schematically shown in Figure 1. PCHMA is unstained by RuO_4.

Image Analysis. NIH image software[13] was used to calculate the statistical sizes of the droplets from the TEM micrographs of the blends. Number-average droplet diameters were calculated. The number of droplets calculated was at least 100 except in the case of 20 min of shearing time at 1 s^{-1} for the systems without bcp in which at least 50 droplets were used to calculate the average droplet sizes. The accuracy of binary thresholded images was checked by comparing with the original images. For nonspherical droplets, diameters were obtained from the areas of ellipsoidal droplets using the equation, area $= \pi(D/2)^2$, where the areas of the droplets were determined by the NIH software. The diameters of some droplets seen on a microtomed section are underestimated, if the section plane does not intersect the droplet center. On the other hand, small particles can be undercounted since the probability of sectioning them is smaller. These potential errors compensate each other, such that the errors in the average droplet size are estimated to be less than 10%; hence, the experimental trends are unaffected by these errors.[5] Therefore, we used the droplet sizes measured by the software directly without correction.

Results and Discussion

Prediction of Stable Droplet Sizes. The Flory−Huggins parameter, χ, was calculated from the indi-

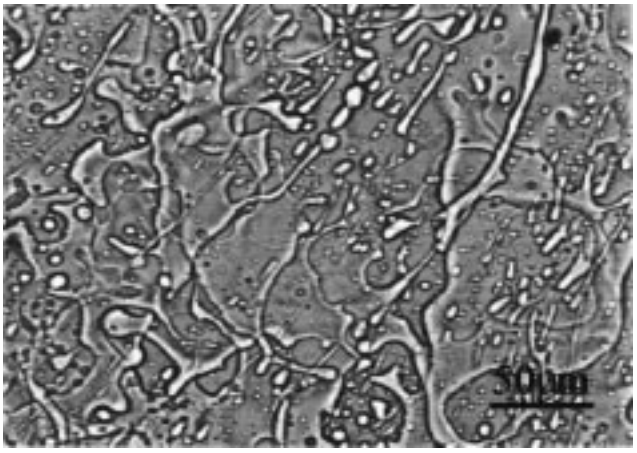

Figure 2. The crude morphology of the SAN33/PCHMA/bcp (5%) before melt mixing with rheometer.

vidual χ parameters of the polymers and the relationship which describes χ for random copolymers.[9]

$$\chi = \chi_{PS-PCHMA}\phi_{PS} + \chi_{PAN-PCHMA}\phi_{PAN} - \chi_{PS-PAN}\phi_{PS}\phi_{PAN} \quad (1)$$

where ϕ_{PS} and ϕ_{PAN} are the volume fractions of styrene and acrylonitrile of the SAN copolymers, respectively. The calculated χ parameters were used to determine the interfacial tensions between SANs and PCHMA using an equation developed from the mean field theory:[14]

$$\Gamma = (\chi/6)^{1/2}\rho_0 b k_B T \quad (2)$$

where Γ is the interfacial tension, ρ_0 is 10^{-2} times Avogadro's number of monomer units/cm^3, b is the effective length per monomer, k_B is Boltzmann's constant, and T is absolute temperature.

The stable droplet diameter of a dispersed phase, subjected to a steady shear rate $\dot{\gamma}$, can be estimated by the Taylor equation[15] determined by the interfacial tension and the shear stress applied:

$$D = \frac{4\Gamma(\eta_r + 1)}{\dot{\gamma}\eta_m\left(\frac{19}{4}\eta_r + 4\right)} \quad (3)$$

where η_r is the relative viscosity of the droplet to the continuous phase and η_m is the viscosity of the continuous phase. However, the Taylor equation is known to be inadequate[16] when η_r is larger than 1; hence, the following empirical fitting relation has been proposed based on Grace's experimental data:[16,17]

$$\log\left(\frac{\eta_m\dot{\gamma}D}{2\Gamma}\right) = -0.506 - 0.0994\log\eta_r + 0.124\log^2\eta_r - \frac{0.115}{\log\eta_r - \log\eta_{r,cr}} \quad (4)$$

where $\eta_{r,cr} = 4.08$ is the critical relative viscosity above which droplet breakup is no longer possible in shear flow. Values of the droplet diameters predicted by eqs 3 and 4 for the SAN33/PCHMA and SAN26/PCHMA systems, respectively, at 50 and at 1 s^{-1} are listed in Table 2, calculated using values of χ, Γ, and the measured apparent viscosity, η, also given in Table 2. Since the viscosity ratios of the present blend systems are around 2, the droplet diameters predicted by the Taylor equation are smaller than those from eq 4.

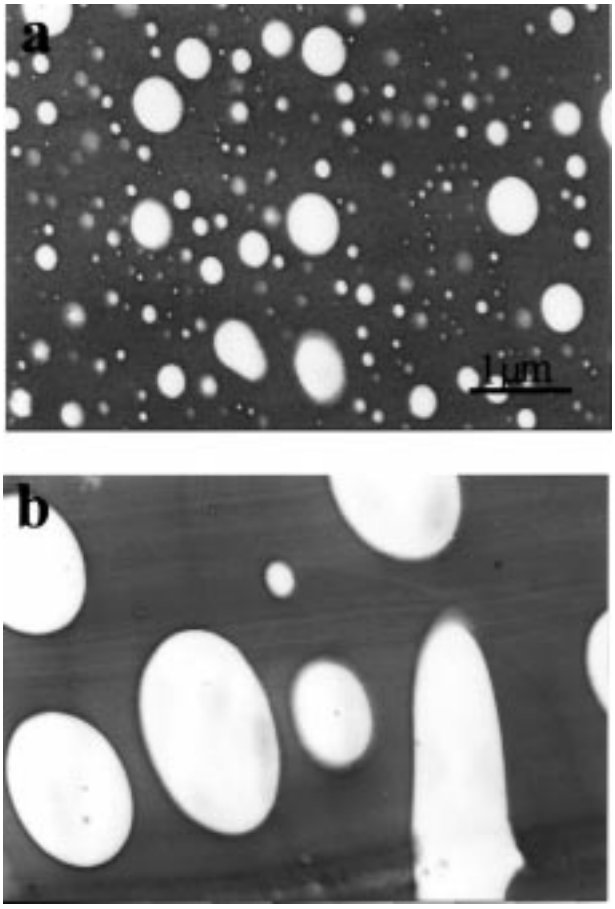

Figure 3. TEM micrographs of SAN33/PCHMA after shearing at 50 s^{-1} for 20 min followed by (a) 0 min and (b) 20 min of shearing at 1 s^{-1}.

An important feature of the results in Table 2 is that the rheological characteristics, η_m, η_d, and η_r, of the blends are very similar; hence, we can expect to isolate the contributions to the coalescence kinetics and morphology evolution of the exothermic mixing interaction between the bcp and the matrix polymers.

Blend Morphology. Optical microscopy of the blend morphology before the shearing process (Figure 2) confirms that the starting morphology is that of a coarse mixture (dispersed phase sizes $\gg 1\ \mu$m) and provides a starting benchmark to characterize the evolution of morphology with shear. TEM micrographs of the modified and unmodified SAN33/PCHMA and SAN26/PCHMA systems are shown in Figures 3−8, and the average droplet sizes from these and other experiments are summarized in Figure 9.

Droplet Breakup and Coalescence without Block Copolymers. The droplet size distributions are similarly polydisperse for both the blend systems after shearing for 20 min at the highest shear rate (50 s^{-1}) (Figures 3a and 4a). Here, the droplet size is determined by breakup of the minor phase. After subsequently applying shear at a low shear rate (1 s^{-1}), where coalescence becomes more important relative to breakup,[8] the droplet sizes in each blend are found to increase with an increasing time of shear (Figure 9). This is clear evidence that coalescence of droplets is occurring. Further, in Figures 3 and 4, it is apparent that most of the smaller droplets disappear rapidly as predicted by

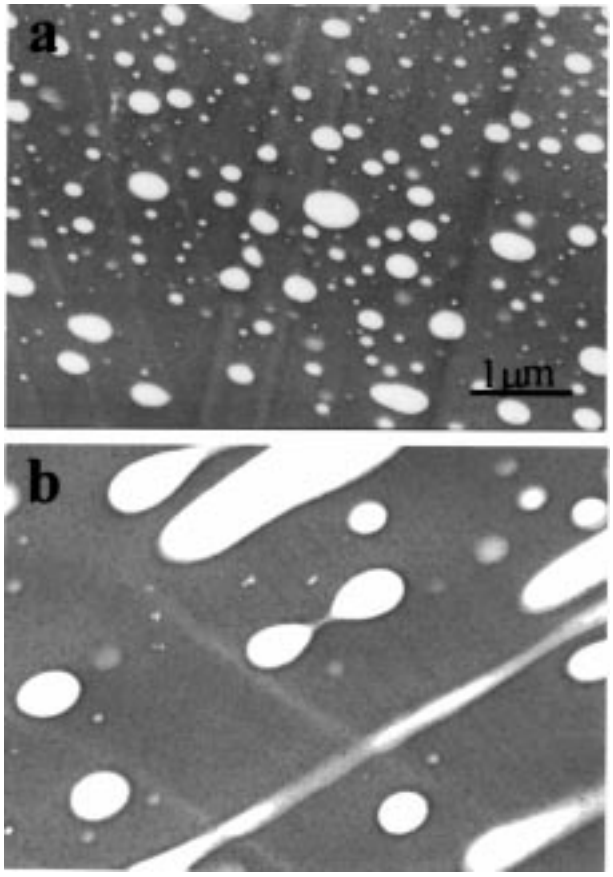

Figure 4. TEM micrographs of SAN26/PCHMA after shearing at 50 s^{-1} for 20 min followed by (a) 0 min and (b) 20 min of shearing at 1 s^{-1}.

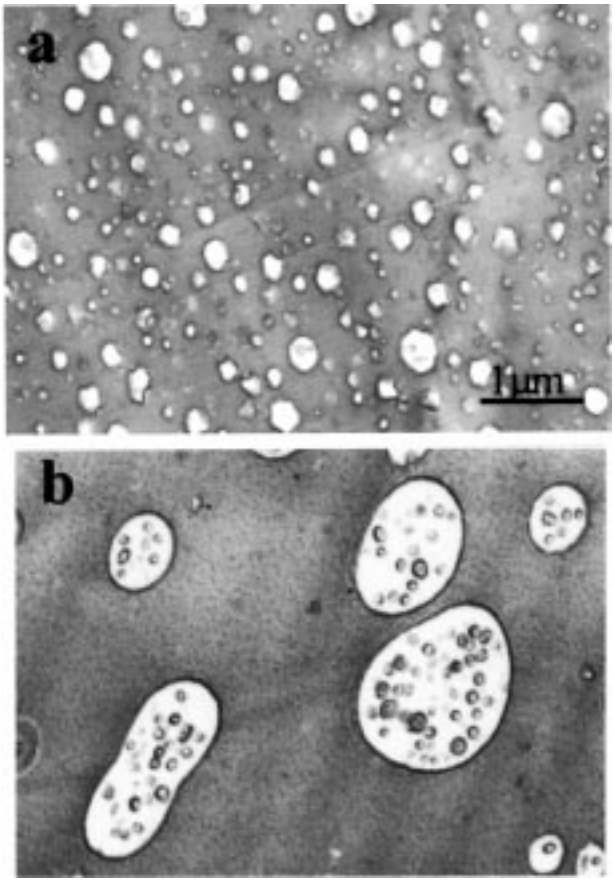

Figure 5. TEM micrographs of SAN33/(PCHMA/2% bcp) after shearing at 50 s^{-1} for 20 min followed by (a) 0 min and (b) 20 min of shearing at 1 s^{-1}.

the coalescence model of Chesters,[7] which indicates small droplets have a higher probability of coalescence.

$$P \sim \exp(-\eta_r \Gamma^{-7/6} D^{13/6} (\dot{\gamma}\eta_m)^{2/3}) \tag{5}$$

Though each blend shows larger droplet sizes with increasing time of low shear, it is visually evident, on comparing Figures 3 and 4, that droplets in the SAN33 blend increase in size more rapidly (Figure 9). Consistent with eq 5, the increased coalescence rate presumably arises from a larger interfacial tension driving force, since the SAN33 blend has a higher interfacial energy at the interface with PCHMA (Table 2).

Droplet Breakup and Coalescence with Block Copolymer. Morphologies of the SAN33/PCHMA/bcp system are shown in Figures 5 and 6 respectively, at two levels of block copolymer content (2% and 5%). The location of the highly stained PS segment of the block copolymer is clearly evident as the darkest features in the micrographs, located at the droplet interface and inside the droplets as micelles. Though much of the block copolymer has migrated to the interface after rapid shearing (Figures 5a and 6a), some block copolymer remains inside the droplets as micelles. A greater fraction of bcp is seen in the interior of larger droplets, which is consistent with the expectation that the homopolymer interface is saturated with bcp. Nevertheless, comparison of Figures 5 and 6 indicates that an increase of block copolymer content to 5% results in a somewhat smaller average droplet size throughout the entire coalescence series of 5, 10, and 20 min at 1 s^{-1} (see Figure 9). When the coalescence condition is applied at a low shear rate, after treatment at a high shear rate, droplet sizes increase abruptly and, again, most of the smaller droplets disappear rapidly as predicted by the coalescence model of Chesters.[7] Here, it is of interest to point out that, recently, Janssen[8] modified Mason's model[18] for fully immobile interfaces and Chesters' model[7] for fully and partially mobile interfaces to obtain simple expressions to predict the probability of coalescence of droplets as a function of the ease of drainage of the fluid between droplets as they approach each other.

For fully mobile interfaces:

$$P_{drain} \sim \exp\{-3/2 \ln(D/2h_{crit})\mathrm{Ca}\} \tag{6}$$

for partially mobile interfaces:

$$P_{drain} \sim \exp\{-\sqrt{3}/2(D/h_{crit})\eta_r \mathrm{Ca}^{2/3}\} \tag{7}$$

and for immobile interfaces:

$$P_{drain} \sim \exp\{-9/2(D/h_{crit})^2 \mathrm{Ca}^2\} \tag{8}$$

where P_{drain} is the probability of drainage of the liquid film between droplets. By combining P_{drain} with the probability of collision between droplets, P_{coll}, we obtain the probability of droplet coalescence, $P_{coal} = P_{drain} \cdot P_{coll}$. Here, P_{coll} is expressed by:

$$P_{coll} = \exp\left(-\frac{t_{coll}}{t_{proc}}\right) = \exp\left(-\frac{\pi}{8\dot{\gamma}\phi t_{proc}}\right) \tag{9}$$

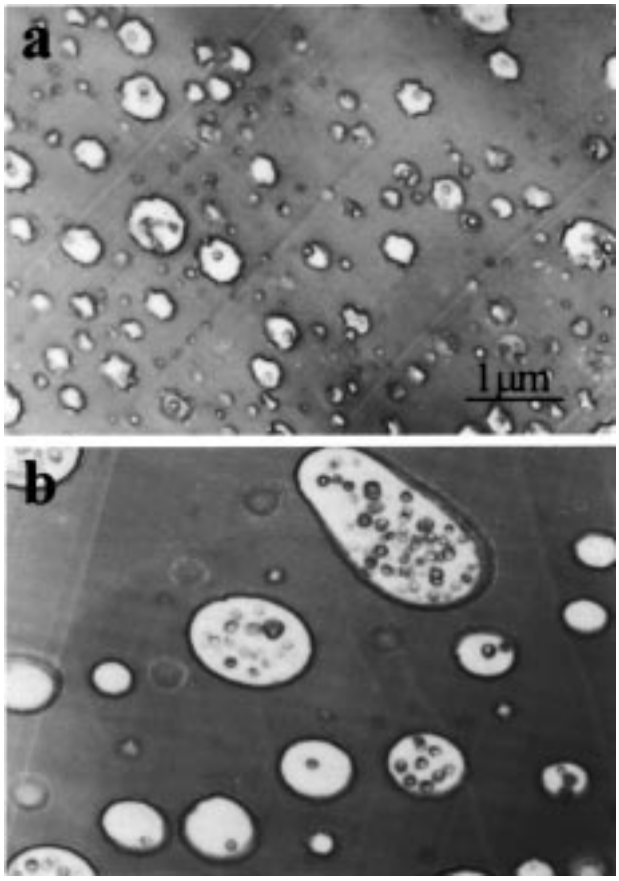

Figure 6. TEM micrographs of SAN33/(PCHMA/5% bcp) after shearing at 50 s^{-1} for 20 min followed by (a) 0 min and (b) 20 min of shearing at 1 s^{-1}.

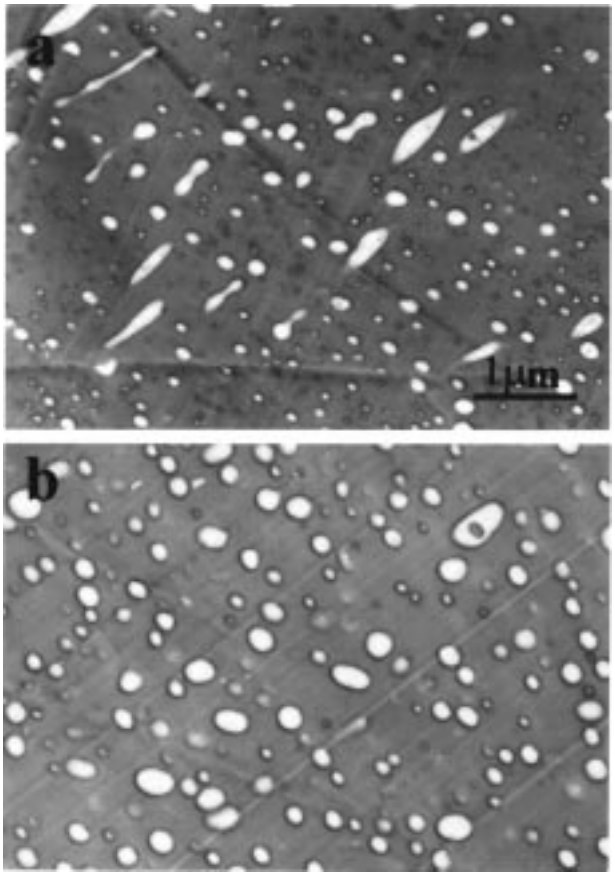

Figure 7. TEM micrographs of SAN26/(PCHMA/2% bcp) after shearing at 50 s^{-1} for 20 min followed by (a) 0 min and (b) 20 min of shearing at 1 s^{-1}.

where t_{coll} is the collision time which is derived from Smoluchowski's equation for collision frequency,[8,19] t_{proc} is the processing time (duration of shear), and ϕ is the volume fraction of the dispersed phase. In eqs 6−8, h_{crit} is the critical distance between two droplets below which the film ruptures abruptly, Ca is the capillary number and is described as $Ca = \dot{\gamma}\eta_m D/\Gamma$. Equations 6−8 indicate that the draining becomes more difficult for immobile interfaces because there is increased friction between the fluid film and the droplet surface. Thus, coalescence is inhibited as the mobility of the interface decreases.

Comparing Figure 3 versus Figures 5 and 6, it is clear on visual inspection that the sizes of coalesced droplets in the presence of block copolymer are smaller than those in the uncompatibilized SAN33/PCHMA system at all times. However, coalescence is clearly evident, despite the addition of block copolymer, and with block copolymer clearly present at the interface between droplets and the matrix. In Figures 7 and 8, we see that the droplet sizes of the PCHMA minor phase in the SAN26 blend containing bcp are much smaller than those of the SAN33/PCHMA/bcp system (cf. Figures 5, 6, and 9) and very little coalescence can be distinguished even after 20 min of coalescence time at the low shear rate even though the collision probability is greater than 0.998 as calculated from eq 9. This very effective inhibition of coalescence is achieved in the SAN26 blend system which has a stronger exothermic interaction between the SAN matrix phase and the PMMA segment of the block copolymer. Increasing block copolymer content from 2% to 5% makes droplet sizes even smaller as can be seen by comparing Figures 7 and 8. Increase of block copolymer concentration results in more block copolymer available at the interface, leading to an increase in interfacial area (i.e., more small droplets) which means that a finer morphology is produced. As for the SAN33/PCHMA/bcp system (Figures 5 and 6), however, the difference in droplet size is relatively small between 2% and 5% bcp, and in each case, the droplet sizes in the compatibilized blend are substantially smaller than the uncompatibilized blends (Figures 3 and 4).

Calculation of the number-average and a type of weight-average droplet sizes (D_n and D_w) was carried out for each blend system using the NIH software. D_n and D_w are defined as

$$D_w = \frac{\sum_N (ND^2)}{\sum_N (ND)} \tag{10}$$

$$D_n = \frac{\sum_N (ND)}{\sum_N N} \tag{11}$$

The values of D_n and the ratio D_w/D_n are shown in Figure 9. Considering first the systems *without* added bcp (i.e., SAN33/PCHMA and SAN26/PCHMA) the experimental analysis indicates, respectively, $D_n = 0.11$ and 0.068 at 50 s^{-1}, and $D_n = 0.69$ and 0.40, respectively, at 1 s^{-1} after 20 min of shear. As is evident in

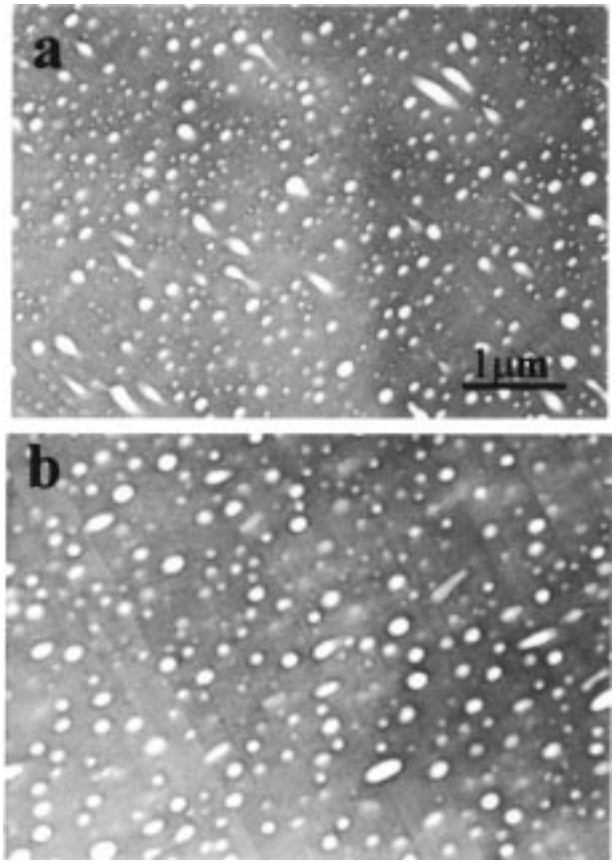

Figure 8. TEM micrographs of SAN26/(PCHMA/5% bcp) after shearing at 50 s^{-1} for 20 min followed by (a) 0 min and (b) 20 min of shearing at 1 s^{-1}.

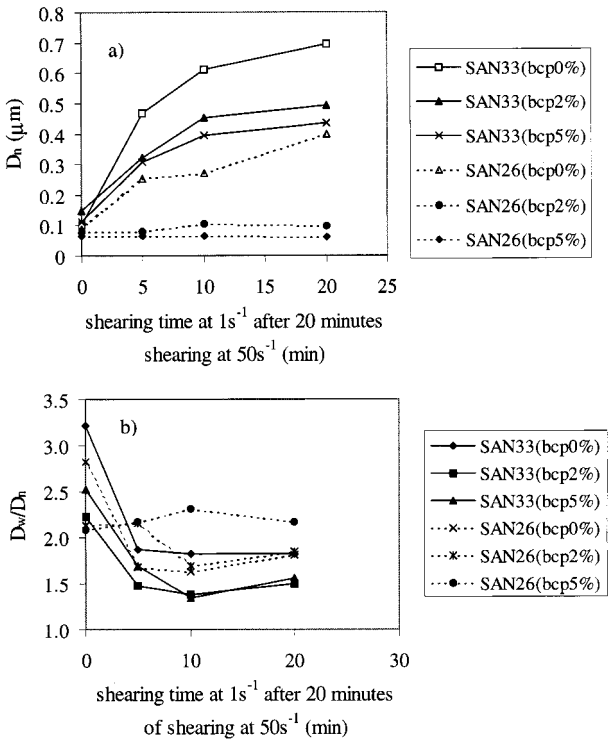

Figure 9. (a) Number-average diameter of droplets; (b) droplet diameter distribution (D_w/D_n) for various blend systems. As evident from Figures 3−8, the size distribution is very polydisperse. The normalized standard deviation is typically $\sigma = \sqrt{\overline{D^2}/(\overline{D})^2 - 1} \approx 40-130\%$, corresponding to $D_w/D_n = 1.4-3.2$.

Table 2, the experimental droplet sizes show variations as a function of shear rate, and between SAN26/PCHMA and SAN33/PCHMA, which are qualitatively consistent with those predicted by either the Taylor equation (eq 3) or the empirical expression (eq 4). Quantitative discrepancies exist. The droplet sizes predicted by eq 4 are closer to the experimental results as expected, since the viscosity ratio $\eta_r \sim 2.0$. Also, in Table 2, it is interesting that the experimental droplet sizes at a high shear rate (50 s^{-1}) are larger by a factor of around 2 than those predicted by eq 4, whereas, at the lower shear rate (1 s^{-1}), the predicted droplet sizes are very close to the experimental data. This observation is in agreement with previous study,[5] which found that the Taylor theory predicts too small droplet sizes for shear-thinning materials because of neglect of polymer elasticity. Thus, the good agreement between prediction and experiment at a low shear rate is consistent with the expectation that there is a relatively low contribution from polymer elasticity at such slow deformations.

The time evolution of D_n (Figure 9a) clearly depicts the inhibitory effect of the block copolymer on coalescence rates, and the fact that an increase of the degree of exothermic interaction between the methyl methacrylate segment of the bcp and the SAN continuous phases acts to enhance the inhibition of coalescence. Comparison of the D_n and D_w values indicates a rapid decrease of the ratio D_w/D_n (Figure 9b), reflecting the initial disappearance of small droplets predicted by Chesters' model of coalescence. The relatively large values of D_w/D_n through the coalescence process reflects that the distributions of droplet sizes are very broad and do not change significantly after the initial rapid decrease. This is clearly consistent with visual inspection of the TEM micrographs (Figures 5−8). The inhibition of coalescence on the addition of bcp is consistent with Chesters' model of coalescence to the extent that addition of the bcp with more exothermic mixing will lower the interfacial tension (cf. eq 5).[20] Such inhibition is also consistent with the expectation that more strongly swollen PMMA segments of the block copolymer on the outer part of the interface make the interface more immobile. An immobile interface provides a lower probability of coalescence compared to a partially or fully mobile interface by increasing the friction at the interface when the fluid film between two droplets drains, as predicted by the equations of Chesters[7] and Janssen (eqs 6−8)[8] At present, we cannot assess the relative importance of the second factor. This will be explored in future work by investigating the dependence of droplet coalescence under a range of shear rates.

Morphology of Solvent Cast Blend. It is useful to compare the morphologies of the melt-mixed blends with those obtained by solvent casting. In Figure 10, we show the morphology of SAN33/PCHMA/bcp and SAN26/PCHMA/bcp blends containing 5% bcp (i.e., the same blend compositions as those shown in Figures 6 and 8, respectively). In the former blend where swelling of the PS segment of block copolymer on the interior side of the minor phase is larger than that of the PMMA segment outside, vesicle shapes are the equilibrium morphology as shown by Adeyinka et al.[1] In contrast, the SAN26 blend, which has stronger swelling of the PMMA bcp segment on the exterior of the minor phase, has spherical domains. Note that the molecular weight of PCHMA is very low compared to that of the SAN

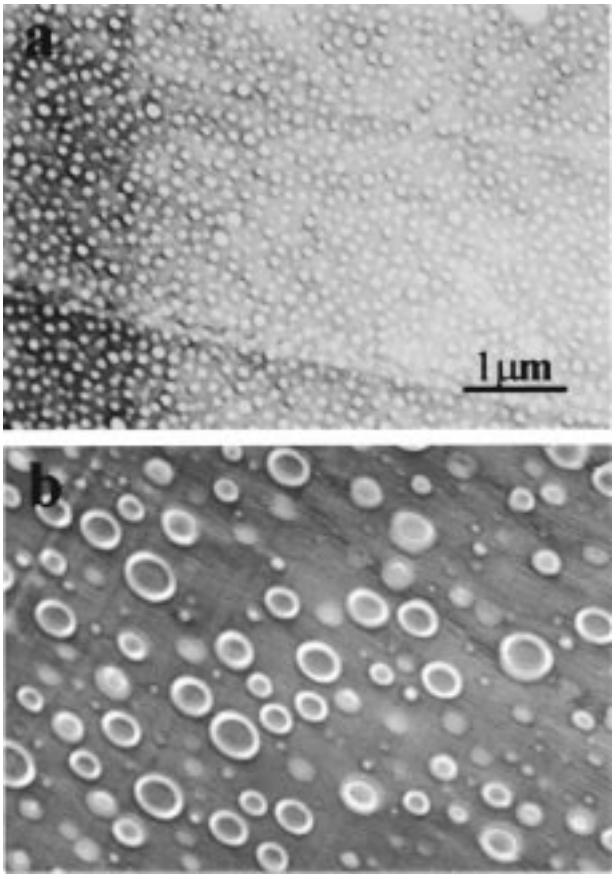

Figure 10. TEM micrographs of solvent-cast blend for (a) SAN26/PCHMA/5% bcp and (b) SAN33/PCHMA/5% bcp.

Table 3. Swelling Factors (*S*) in SAN*x*/PCHMA/bcp Blends

	SAN33/PCHMA/bcp	SAN26/PCHMA/bcp
P (SAN)[a]	764.9	756.3
P (PCHMA)[a]	216.3	216.3
N (b-PMMA)[a]	1548	1548
N (b-PS)[a]	1381	1381
χ (SANx/PMMA)	−0.00048	−0.00928
χ (PCHMA/PS)	−0.00319	−0.00319
S (SANx/PMMA)	3.49	30.8
S (PCHMA/PS)	15.2	15.2

[a] N and P are calculated on the basis of the number-average molecular weight.

copolymer, and hence the PS segments of the block copolymer at the inner interface can be swollen to a degree larger than the exothermically assisted swelling of the PMMA segment by SAN33 at the outer interface, but not as strongly as the swelling of PMMA by SAN26.

These ideas can be quantified through calculation of the theoretical swelling factors S expressed as[21,22]

$$S = -2\chi N + N/P \qquad (12)$$

where χ is the Flory−Huggins parameter and N and P are the degrees of polymerization of the block copolymer and the homopolymer, respectively. Using the relevant values of χ, N and P listed in Table 3, we calculate the values of S for the swelling of the *b*-PMMA brush by SAN, and the *b*-PS brush by PCHMA, also given in Table 3. Table 3 indicates that the swelling between PCHMA and *b*-PS ($S = 15.2$) is much larger than that between SAN33 and *b*-PMMA ($S = 3.49$), consistent with the vesicle morphology in the SAN33/PCHMA/bcp blend (Figure 10b). In contrast, from Table 3, the swelling between PCHMA and *b*-PS ($S = 15.2$) is substantially smaller than that between SAN26 and *b*-PMMA ($S = 30.8$), consistent with the spherical droplet morphology in the SAN26/PCHMA/bcp blend (Figure 10a).

The melt-blended SAN 26 system maintains its small droplet size throughout the droplet breakup and coalescence process since the high shear treatment produces a near equilibrium morphology (compare Figures 8a and 10a). In contrast, the equilibrium morphology of SAN33 consists of vesicle structures, which means that the sphere morphology produced by high shear is not stable, increasing the tendency for coalescence. Thus, we expect to find a correlation between block copolymer swelling factors and morphology of melt-mixed immiscible blends compatibilized by a block copolymer. This will be explored in future work.

Conclusion

In this study, morphology of immiscible blends was investigated under simple shear, which facilitates interpretation in terms of droplet breakup and coalescence, and avoids the complex deformation history encountered in commercial mixing processes. Using the blend system of SAN/PMMA-*b*-PS/PCHMA, it was possible to identify the location of the added block copolymer by selectively staining the bcp PS segment. As a result, we found that a portion of block copolymers diffuses to the interface while the remainder stays inside the droplets as swollen micelles. By choosing blend components of similar molecular weights, and having similar viscosities, the influence of exothermic interaction between the continuous phase and the PMMA segment of the block copolymer was investigated by utilizing a SAN random copolymer as the continuous phase, and changing the AN content of the SAN.

Increasing the exothermic interaction between SAN and PMMA results in smaller droplet sizes by more effective inhibition of coalescence. Morphological analysis of melt-blended specimens was carried out to evaluate the blend morphology under high shear mixing and then the coalescence and morphology evolution under low shear. Addition of bcp decreased droplet sizes for both SAN33/bcp/PCHMA and SAN26/bcp/PCHMA systems at high shear. In the SAN33 blend containing bcp, coalescence occurs at a rate similar to that in the absence of bcp. In the SAN26 blend, droplet sizes under high shear were very small, comparable to the equilibrium morphology, and coalescence was virtually absent. The effect on coalescence is consistent with the expectation that the exothermic interaction between the bcp brush and the matrix influences droplet sizes via thermodynamic control (lowering of interfacial tension) and dynamically by producing a more rigid interface.

Acknowledgment. We are grateful to the Edison Polymer Innovation Corp. and the General Electric Co. for financial support of this work.

References and Notes

(1) Adeyinka, A.; Jamieson, A. M.; Hudson, S. D. *Macromol. Chem. Phys.* **1996**, *197*, 2521.
(2) Adeyinka, A.; Jamieson, A. M.; Hudson, S. D. *Polymer* **1997**, *38*, 737.
(3) Wang, Z. G.; Safran, S. A. *Europhys. Lett.* **1990**, *11* (5), 425.
(4) Tan, N. C. B.; Tai, S.-K.; Briber, R. M. *Polymer* **1996**, *37*, 3509.

(5) Sundararaj, U.; Macosko, C. W. *Macromolecules* **1995**, *28*, 2647.
(6) Milner, S. T.; Xi, H. *J. Rheol.* **1996**, *40*, 663.
(7) Chesters, A. K. *Trans. I Chem. E.* **1991**, *69A*, 259.
(8) Janssen, J. M. H. Dynamics of Liquid−Liquid Mixing. Ph.D. Thesis, Eindhoven University of Technology, Eindhoven, 1993; pp 59−75.
(9) Nishmoto, M.; Keskkula H.; Paul, D. R. *Macromolecules* **1990**, *23*, 3633.
(10) Wu, S. *Polym. Eng. Sci.* **1987**, *27*, 335.
(11) Chen, C. C.; White, J. L. *Polym. Eng. Sci.* **1993**, *33*, 923.
(12) Taha, M.; Frerejean, V. *J. Appl. Polym. Sci.* **1996**, *61*, 969.
(13) NIH image software is available on the Internet, http://rsb.info.nih.gov/nih-image/.
(14) Helfand E.; Tagami, Y. *J. Chem. Phys.* **1972**, *56*, 3592.
(15) Taylor, G. I. *Proc. R. Soc. London* **1934**, *A146*, 501.
(16) Grace, H. P. *Chem. Eng. Commun.* **1982**, *14*, 225.
(17) Minale, M.; Mewis J.; Moldenaers, P. *AIChE J.* **1982**, *44*, 943.
(18) Mackay, G. D.; Mason, S. G. *Can. J. Chem. Eng.* **1963**, 41, 203.
(19) Smoluchowski, M. *Z. Phys. Chem.* **1917**, *92*, 129.
(20) Dai, K. H.; Kramer, E. J.; Shull, K. R. *Macromolecules* **1992**, *25*, 220.
(21) Braun, H.; Rudolf, B.; Cantow, H. J. *Polym. Bull.* **1994**, *32*, 241.
(22) Adeyinka, A.; Hudson, S. D.; Jamieson, A. M. *Polymer* **1997**, *38*, 737.

MA971888N